A Hybrid Tracking Algorithm for Multistatic Passive Radar

Kan Shu, Jianxin Yi, *Member, IEEE*, Xianrong Wan, and Feng Cheng

***Abstract*—In multistatic passive radars (MPR), multiple measurements from different bistatic pairs are usually used to locate the target due to the inaccurate direction of arrival estimation. In the real-world scenarios, the available bistatic pairs may be not enough and the probability of detection for each bistatic pair may be relatively low. It cannot be guaranteed that multiple simultaneous measurements will be available. In this case, the existing tracking algorithms face problems in the fast track confirmation, track continuity, and accuracy. In this article, we propose a novel hybrid tracking algorithm for the MPR. To handle the above-mentioned problems, we construct two classes of tracks, namely the high-precision track and low-precision track, for both the track initialization and track maintenance stages. The low-precision track can be converted into the high-precision track under certain conditions. This design facilitates the fast confirmation of high-precision tracks. Combined with the independent management of the high-precision tracks, the track continuity and accuracy metrics will be enhanced as well. The superiority of the proposed algorithm is validated via theoretical analyses and Monte Carlo simulations. Moreover, the experimental results using real data also demonstrate the practical effectiveness.**

***Index Terms*—Hybrid tracking, multistatic passive radar (MPR), target tracking, track initialization, track maintenance.**

I. Introduction

THE target information obtained by a bistatic passive radar [1]–[4] is relatively limited, leading to the deficiency in the localization accuracy, detection probability, coverage area, and other aspects. An alternative solution to this problem is the multistatic passive radar (MPR) [5]–[8]. The MPR consists of multiple transmitter-to-receiver pairs (i.e., bistatic pairs) that may come from multiple noncooperative transmitters, or multiple receivers, or both. It has the potential to extract more precise features of the target through information fusion across multiple bistatic pairs. This article concerns the information fusion problem in the target tracking for the MPR.

Manuscript received December 11, 2019; revised April 3, 2020 and May 6, 2020; accepted May 8, 2020. Date of publication May 25, 2020; date of current version June 16, 2021. This work was supported in part by the National Natural Science Foundation of China under Grants 61701350 and 61931015, in part by the National Key R&D Program of China under Grant 2016YFB0502403, in part by the Postdoctoral Innovation Talent Support Program of China under Grant BX201600117, in part by the Technological Innovation Project of Hubei Province of China under Grant 2019AAA061, and in part by the Fundamental Research Funds for the Central Universities under Grant 2042019kf1001. *(Corresponding author: Jianxin Yi.)*

The authors are with the School of Electronic Information, Wuhan University, Wuhan 430000, China, and also with the Collaborative Innovation Center for Geospatial Technology, Wuhan 430000, China (e-mail: kanshu@whu.edu.cn; jxyi@whu.edu.cn; xrwan@whu.edu.cn; cwing@whu.edu.cn).

Digital Object Identifier 10.1109/JSYST.2020.2994009

In the past four decades, a variety of architectures are available for the design of a multisensor tracking system [9], [10]. The main ideas of these tracking system can be grouped into two categories: state vector fusion and measurement fusion. The state vector fusion method [11]–[14] combines the filtered state vectors from different sensors to form a new estimate while the measurement fusion method [15]–[18] directly fuses measurements produced by different sensors. A comparison of these two methods can be found in [19].

The state vector fusion method requires each sensor to process its own measurements and keep its tracks separately. However, for the MPR, the direction of arrival (DOA) estimation is usually inaccurate, which results in a significant deviation in the tracks. Besides, complex clutter environments cause lots of false tracks. These inaccurate tracks and false tracks pose a great challenge to the track-to-track association and the track fusion.

To overcome the above-mentioned problems, the measurement fusion method is considered for the MPR. In the MPR, one bistatic range defines an ellipse/ellipsoid with the foci at the corresponding transmitter and receiver positions. Intercepting multiple ellipses/ellipsoids from multiple bistatic pairs make the target localization possible [20]–[24]. Further considering that the bistatic ranges are usually of high accuracy, it is attractive and popular to fuse multiple bistatic range measurements in the MPR.

Several multitarget tracking methods based on the measurement fusion have been proposed in [25]–[28] for the MPR. In [25], each track is initialized using at least three bistatic pairs. A nonlinear Kalman filter is then used to update tracks. This nonlinear Kalman filter makes it possible to update 3-D tracks with only one or two simultaneous detections. Such an idea is also used in [26]. Combined with the 2-D assignment method, the problem in the track maintenance stage under a single frequency network (SFN) can be solved. Both [25] and [26] do not provide a detailed description of the track initialization. Yi *et al.* [27] proposes an approximately optimal assignment method to solve the association problem among targets, measurements, and illuminators. The target's Cartesian position and velocity, namely secondary measurement, can be estimated after the association operation. The secondary measurements are then used to update tracks in the Cartesian coordinate. Choi *et al.* [28] present the auxiliary particle filter and the bootstrap particle filter under the probabilistic multihypothesis tracker (PMHT) measurement model for a DAB/DVB network.

The above-mentioned measurement fusion methods could work well if there are sufficient bistatic pairs and high detection

probability. But in the real-world scenarios, the multiple simultaneous measurements for the same target may not be guaranteed due to the insufficient bistatic pairs and low detection probability. In this scenario, the probability of obtaining a secondary measurement is reduced. Thus, the above-mentioned tracking algorithms encounter difficulties in the fast track confirmation, track continuity, and accuracy.

The objective of this article is to improve the tracking performance in the case of insufficient bistatic pairs and low detection probability. We propose a novel hybrid tracking algorithm for the MPR. The key to the proposed algorithm is that two classes of tracks, namely the high-precision track and low-precision track, are constructed. Unlike the above-mentioned tracking algorithm, the target information detected by only one bistatic pair is saved in the low-precision tracks instead of being directly discarded. After the association between low-precision tracks and the secondary measurement, the associated low-precision tracks are converted into a high-precision track. This design directly increases the probability of the high-precision track confirmation. Meanwhile, to make it possible to update tracks with one detection, a nonlinear Kalman filter is used in the track maintenance stage. In addition, combined with the independent management of the high-precision tracks, the track continuity and accuracy metrics will be enhanced as well. Monte Carlo (MC) simulations and theoretical derivation are used to evaluate the performance of the proposed algorithm. Its practical effectiveness is further verified using real data.

The rest of this article is organized as follows. Section II describes the difficulties in the target localization and track initialization in the case of insufficient bistatic pairs and low detection probability. Then, the proposed algorithm is described in Section III. Section IV evaluates the performance of the proposed algorithm through theoretical derivation and simulations. Section V demonstrates the performance using field experimental data. Finally, concluding remarks are drawn in Section VI.

II. Problem Formulation

Consider a MPR system with N_t transmitters and N_{r} receivers. It is assumed that all the transmitters' and receivers' positions are known. A transmitter and a receiver form a bistatic pair. In the considered case, there are $N = N_{\mathrm{t}} \times N_{\mathrm{r}}$ bistatic pairs. Let $\boldsymbol{x}(t)$ and $\boldsymbol{Z}_n(t) = \{\boldsymbol{z}_n^{(1)}(t), \boldsymbol{z}_n^{(2)}(t), \cdots, \boldsymbol{z}_n^{(M_n)}(t)\}$ be the target state and the measurements of bistatic pair$n (n = 1, 2, \cdots, N)$, respectively, where M_n denotes the number of measurements in the nth bistatic pair. The timestamp t may be omitted under unambiguous situation. The relationship between the target and the m_nth$(m_n = 1, 2, \cdots, M_n)$ measurement can be expressed as

$$\boldsymbol{z}_n^{(m_n)} = \begin{bmatrix} r_b \\ v_b \\ \theta \end{bmatrix} = \begin{cases} \boldsymbol{h}_n(\boldsymbol{x}) + \boldsymbol{w}_n & \text{if target measurement} \\ \tilde{\boldsymbol{z}} & \text{if false alarm} \end{cases} \tag{1}$$

where $\boldsymbol{h}_n(\cdot)$is the measurement function associated with bistatic pair n, and w_n is the measurement noise. The measurement consists of the bistatic range r_{b}, bistatic velocity v_{b}, and azimuth θ. Without loss of generality, it is assumed that all the measurement noises of different bistatic pairs are independently and identically distributed (i.i.d.), with covariance matrix $\boldsymbol{R}$.

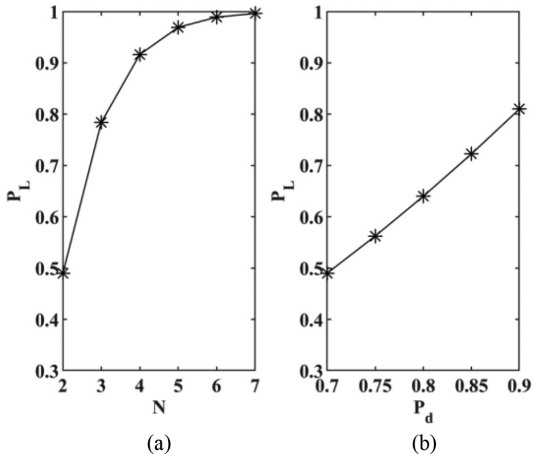

Fig. 1. Results of P_{L}. (a) P_{L} varies with the number of bistatic pair N when $P_d = 0.7$. (b) P_{L} varies with the detection probability P_d when $N = 2$.

In current passive radar systems, multiple measurements from different bistatic pairs are usually used to locate the target due to the inaccurate DOA estimation. At least two different bistatic ellipses are needed to locate the target in the case of 2-D space. When faced with a situation where the bistatic pair is insufficient and the detection probability is low, the probability that the target can be located, denoted by P_L, is reduced. P_L can be expressed as the function of the detection probability and the number of bistatic pairs. For description brevity, we assume that all the bistatic pairs have the same detection probability P_d. The probability P_L can then be calculated as

$$P_L = \sum_{i=2}^{N} C_N^i {P_d}^i (1 - P_d)^{N-i} \tag{2}$$

where C_N^i is the number of combinations of *i* selected from *N*.

Fig. 1 shows the P_L calculated under various N and P_d. As it is depicted, P_L is less than 0.8 when the number of bistatic pairs is small (three or less), or the detection probability is low. If we only use the multistatic localization results to initialize tracks, it will result in a low probability of new track confirmation. The reason is intuitive. In the multistatic localization, the target can only be located when it is simultaneously detected by two or more bistatic pairs. The target measurement detected by only one bistatic pair is directly discarded. In order to make full use of all bistatic measurements, we introduce the concept of high-precision track and low-precision track and propose a hybrid tracking algorithm based on these two kinds of tracks in this article.

III. Proposed Hybrid Tracking Algorithm

As shown in Fig. 2, the original measurements of each bistatic pair serve as the input of the multistatic hybrid tracking. In the multistatic hybrid tracking we introduce the concept of

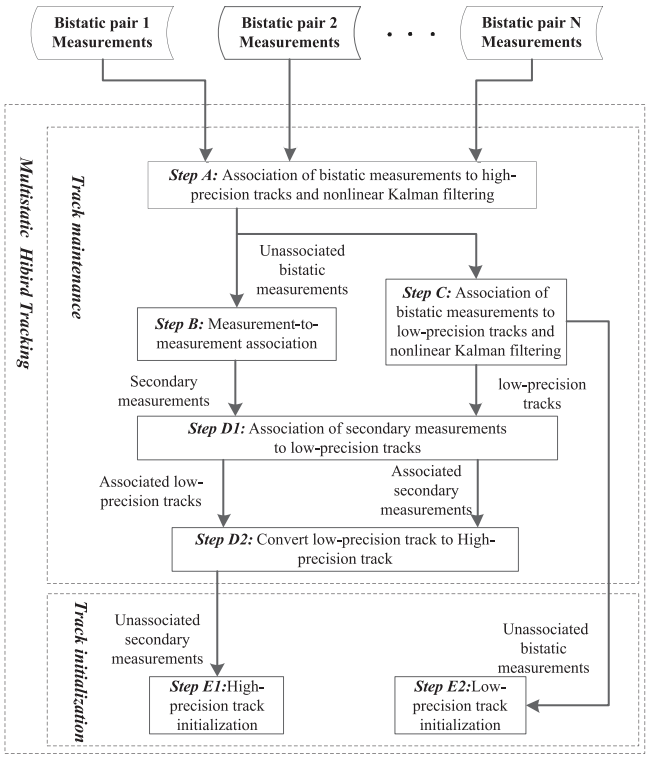

Fig. 2. Block diagram of the proposed algorithm.

high-precision and low-precision track. The low-precision track refers to the track formed by the measurements of each single bistatic pair. The high-precision track is a track that is directly initialized by a secondary measurement sequence or that is obtained by the fusion of low-precision tracks associated with the same secondary measurement. It should be emphasized that the low-precision tracks are confirmed tracks, not tentative tracks. If there is no more information to convert these low-precision tracks into high-precision tracks, they will be considered as target tracks instead of being deleted.

There are two modules in the tracking process, namely the track maintenance and track initialization. The track maintenance module mainly consists of the measurement-to-measurement association, the conversion from low-precision tracks to the high-precision track, and the track update processes for both high-precision tracks and low-precision tracks. These key steps will be detailed below. The track initialization module is mainly used to initialize and confirm new tracks in both classes of tracks.

The main difference between the proposed algorithm and existing MPR tracking algorithms is that we have added a branch related to low-precision tracks after the high-precision track filtering. The role of this additional branch is to preserve the target measurements obtained by all the bistatic pairs, including those discarded in the measurement-to-measurement association step. After the measurement-to-measurement association, the low-precision tracks and the secondary measurement that represent the same target are associated with each other under certain conditions. Then, we convert the low-precision tracks and the associated secondary measurement to a high-precision track. Such design can increase the probability of high-precision track confirmation. Moreover, combined with the independent management of the high-precision tracks, the track continuity and accuracy metrics will be enhanced as well. In the proposed algorithm, both the measurement-to-measurement association and the low-precision track update impose a one-to-one constraint. There is no case where the same low-precision track is associated with multiple secondary measurements.

A. High-Precision Track Update

In Fig. 2, the high-precision track update is marked as step A. This step is mainly about the measurement-to-track association and the high-precision track update. Let $\boldsymbol{X}_H(t) = \{\boldsymbol{x}_H^{(1)}(t), \ldots, \boldsymbol{x}_H^{(\lambda)}(t)\}$ be the state of all the high-precision tracks, where λ is the number of high-precision track at time t. If $\lambda = 0$, it means there is no high-precision track at this time, then skip to the next step directly. Since bistatic pairs are independent of each other, the measurement-to-track association can be performed in each bistatic pair individually. For example, in the nth bistatic pairs, the association problem between the high-precision tracks $\boldsymbol{X}_H(t)$ and the measurements $\boldsymbol{Z}_n(t)$ can be transformed into a 2-D assignment problem. It can be solved by the Hungarian algorithm [26]. This operation is repeated for all bistatic pairs. Let $\boldsymbol{Z}^{(j)}(t) = [\boldsymbol{z}_1^{(m_1)}(t), \boldsymbol{z}_2^{(m_2)}(t), \cdots, \boldsymbol{z}_N^{(m_N)}(t)]$ denote the measurements from all the bistatic pairs associated with $\boldsymbol{x}_{\mathrm{H}}^{(j)}(t)$, where $j \in \{1, 2, \cdots, \lambda\}$. An extended Kalman filter is then used to update the high-precision track due to the highly nonlinear between $\boldsymbol{Z}^{(j)}(t)$ and $\boldsymbol{x}_{\mathrm{H}}^{(j)}(t)$. The detailed process of using EKF to update the target status can be found in [31]. With such an efficient nonlinear filter, it is possible to update tracks with only one measurement.

In order to avoid track duplication, the measurements associated with high-precision tracks will be deleted after high-precision track filtering. The remaining measurements are taken as the inputs of both step B and step C. The inputs for step B and C are exactly the same.

B. Measurement-to-Measurement Association

In Fig. 2, this part is marked as step B. The purpose of this step is to find the measurements from different bistatic pairs that represent the same target. At the same time, we obtain the secondary measurement mentioned in Section I by fusing these measurements and record the indexes of these measurements in a 2-D matrix. We use the method introduced in [27] to deal with this problem. The method in [27] is originally proposed for the MPR with an SFN. It is also applicable to the general MPR system. The method can be briefly described as follows.

1) Take two measurements from two bistatic pairs to construct a low-dimensional association hypothesis.
2) Given association probability P_{Ass}, make a quick decision on all the association hypotheses constructed in step 1.
3) Fuse the association hypotheses accepted in step 2 and further collate them into candidate target groups.

4) Reallocate the association between the measurements and the candidate targets by the global association model. At the same time, the target's Cartesian position and velocity, namely the secondary measurement are obtained.
5) Record the composition of the secondary measurement.

It should be noted that the association probability P_{Ass} is a user-defined parameter, which is discussed in [32].

Let $\boldsymbol{z}_{\mathrm{snd}}^{\beta}(t)$ and P_{snd}^{β} denote the target state and covariance matrix of the βth secondary measurement at time$t$, respectively. The composition of the secondary measurement is recorded as

$$\boldsymbol{T}_{\beta}(t)=\begin{bmatrix}\cdots & n & \cdots\\ \cdots & m_n & \cdots\end{bmatrix}_{2\times p} \tag{3}$$

which is a $2\times p$ matrix and p is the number of bistatic pairs that compose the secondary measurement. In the matrix, the first row of each column stores the index of the bistatic pair n, and the second row indicates the index of the measurement in the corresponding bistatic pair m_n. For example, the composition of one secondary measurement is as follows: the first measurement in the first bistatic pair, the fourth measurement in the second bistatic pair, and the third measurement in the fourth bistatic pair. The composition of this secondary measurement can then be recorded as

$$\boldsymbol{T}_1=\begin{bmatrix}1 & 2 & 4\\ 1 & 4 & 3\end{bmatrix}. \tag{4}$$

C. Low-Precision Track Update

In Fig. 2, this part is marked as step C. The association between the low-precision tracks and measurements is carried out in the bistatic coordinates. We also formulate the association problem between tracks and measurements into a 2-D assignment problem and solve it using the Hungarian algorithm. Meanwhile, the index of the measurement associated with the track is recorded. A nonlinear filter is then used to update low-precision tracks [33].

We use $l_q(t)$ to indicate the number of low-precision tracks in the $q\mathrm{th}(q=1,2,\cdots,N_{T-R})$ bistatic pair at time t. There are a total of $l(t)=\sum_{q=1}^{N_{T-R}} l_q(t)$ low-precision tracks in all bistatic pairs. We define a matrix $L(t)$ with two rows and $l(t)$ column:

$$\boldsymbol{L}(t)=\begin{bmatrix}\cdots & n & \cdots\\ \cdots & m_n & \cdots\end{bmatrix}_{2\times l(t)}. \tag{5}$$

Each column in the first row of $\boldsymbol{L}(t)$ indicates the index of the bistatic pair where the low-precision track is located. The corresponding element in the second row denotes the index of the measurement associated with the track.

D. Low-Precision Track Conversion

In Fig. 2, this part is marked as step D1 and step D2. In step D1, we associate low-precision tracks with secondary measurements. It is conducted as follows. For each secondary measurement, e.g.,$\boldsymbol{z}_{\mathrm{snd}}^{\beta}(t)$, we compare all the columns in the matrix $\boldsymbol{L}(t)$ with each column of $\boldsymbol{T}_{\beta}(t)$. Record the number of identical columns as n_{col}^{β}. There are three cases for n_{col}^{β}.

1) If $n_{\mathrm{col}}^{\beta}>1$, it indicates that there are multiple low-precision tracks associated with $\boldsymbol{z}_{\mathrm{snd}}^{\beta}(t)$. We claim that these low-precision tracks and the secondary measurement correspond to the same target.
2) If $n_{\mathrm{col}}^{\beta}=1$, it indicates that only one low-precision track is associated with $\boldsymbol{z}_{\mathrm{snd}}^{\beta}(t)$. To guarantee the reliability of the association, an extra judgment is added to further confirm whether the secondary measurement and the low-precision track correspond to the same target. Let $\boldsymbol{x}_l$ and P_{low} denote the state and covariance matrix of the low-precision track. We calculate the square of the following Mahalanobis distance and do the decision

$$d_{\beta}^2=(\boldsymbol{x}_l-\boldsymbol{z}_{\mathrm{snd}}^{\beta})^T(P_{\mathrm{low}}+P_{\mathrm{snd}}^{i})^{-1}(\boldsymbol{x}_l-\boldsymbol{z}_{\mathrm{snd}}^{\beta})\underset{\text{accept}}{\overset{\text{reject}}{\lessgtr}}\mu \tag{6}$$

where μ is the decision threshold obtained by a given probability. The square of the Mahalanobis distance d_{β}^2 approximately follows the chi-square distribution with degree-of-freedom$2\times D$, where *D* represents the spatial dimension, i.e., $d_{\beta}^2\sim\chi^2(2\times D)$. μ is the upper quantile of this chi-square distribution, usually calculated according to the 95% confidence interval. When $d_{\beta}^2<\mu$, the secondary measurement $\boldsymbol{z}_{\mathrm{snd}}^{\beta}(t)$ and the low-precision track correspond to the same target. Otherwise, we draw the contrary conclusion.

1) If $n_{\mathrm{col}}^{\beta}<1$, it indicates that there is no low-precision track associated with $\boldsymbol{z}_{\mathrm{snd}}^{\beta}(t)$.

In step D2, if there are low-precision tracks associated to secondary measurement $\boldsymbol{z}_{\mathrm{snd}}^{\beta}(t)$, we further convert these low-precision tracks into a high-precision track. In practical applications, the merged state obtained by track fusion method is usually bad due to the inaccuracy of low-precision tracks. In addition, there may be only a single low-precision track associated with the secondary measurement. On the other hand, note that the secondary measurement is quite accurate in the position and velocity. Thus, we directly use the secondary measurement $\boldsymbol{z}_{\mathrm{snd}}^{\beta}(t)$ as the state of the first point of the high-precision track. The corresponding covariance matrix is P_{snd}^{β}. At the same time, terminate those n_{col}^{β} low-precision tracks.

The above operations are repeated for all the secondary measurements.

E. Track Initialization

In Fig. 2, this part is marked as step E1 and step E2. After processing by the track maintenance module, those measurements that are not related to all the existing tracks, including bistatic measurements and secondary measurements, are considered as new targets or false alarms. We can then initialize new tracks and eliminate false alarms by standard algorithms (e.g., *M/N* logic-based track initialization (LBTI) algorithm [29]) for both high-precision track and low-precision track in both step E1 and E2. It should be noted that the high-precision track and low-precision track that are successfully initialized at this time may correspond to the same target. But in the subsequent cycles, the high-precision track will be preferentially associated with the bistatic measurements in step A, so that the low-precision track

corresponding to the same target in step C will be terminated because there is no more measurement associated with it. This operation avoids the case where the high-precision track and the low-precision track correspond to the same target are both in the output.

IV. Performance Evaluation

In this section, we will verify the performance of the proposed algorithm in terms of the fast track confirmation, track continuity, and accuracy. Only the 2-D space is considered in the following discussion.

A. Probability of High-Precision Track Confirmation

This part will quantitatively analyze the performance of the proposed algorithm in terms of the fast track confirmation by theoretical derivation and simulations. The LBTI algorithm will be used as a reference. It directly uses the multiframe secondly measurements to initialize tracks.

We use the probability of high-precision track confirmation as an indicator to measure the performance of the fast track confirmation. It refers to the possibility that the track is confirmed successfully in the specified number of frames. For simplicity, we consider the simple case of the 2/2 LBTI method, where the track will be confirmed if the target is detected and associated in two consecutive frames. The algorithm proposed in [27] is used to obtain the secondary measurement. The association probability mentioned in step 2 of Section IV-B is denoted as P_{Ass}. We set the same track-to-measurement association threshold in both high-precision tracks and low-precision tracks. A given probability, denoted by $P_{\mathrm{Threshold}}$, is used to obtain this track-to-measurement association threshold.

To calculate the high-precision track confirmation probability of the 2/2 LBTI method and the proposed algorithm, respectively, we define the following five events first.

Event A_i: the target that is simultaneously detected by $i(i \geq 2)$ bistatic pairs.

Event B_k: the target is simultaneously detected by i bistatic pairs, but the number of bistatic pairs that make up the secondary measurement is $k(2 \leq k \leq i)$.

Event C_k: in the k bistatic pairs that make up the secondary measurement, at least one bistatic pair successfully initiates a low-precision track.

Event D_i: the target is simultaneously detected by i bistatic pairs, and at least one of the bistatic pairs that constitute the secondary measurement has successfully initiated the low-precision track.

Event E_i: the secondary measurement is not associated with the low-precision track, and it is not converted to a high-precision track.

Using $P(A_i)$,$P(B_k)$,$P(C_k)$,$P(D_i)$, and $P(E_i)$ to indicate the probability of occurrence of events A_i, B_k, C_k, D_i, and E_i, respectively.

Then, the probability P_L defined in Section II can be expressed as follows:

$$P_L = \sum_{i=2}^{N} P(A_i). \tag{7}$$

Assuming that each association hypothesis is independent, $P(A_i)$ can be approximately calculated as follows:

$$P(A_i) \approx C_N^i {P_d}^i (1-P_d)^{N-i} (1-(1-P_{Ass})^{C_i^2}). \tag{8}$$

The probability of track confirmation using the 2/2 LBTI method can then be expressed as follows:

$$P_{\mathrm{Init-LBTI}} = P_L^2 P_{\mathrm{Threshold}}. \tag{9}$$

Next, we calculate the probability of high-precision track confirmation of the proposed algorithm. The calculation is divided into three steps.

1) Probability of Converting Low-Precision Tracks Into High-Precision Track: The measurements from k bistatic pairs that make up the secondary measurement involve a total of C_k^2 association hypotheses. In fact, not all association hypotheses are independent of each other. Some association hypotheses that contain the same measurement from the same bistatic pair are correlated, which makes it difficult to accurately calculate the probability of event B. Hence, it is necessary to take some approximation to calculate the probability of event B. Here, we assume that all association hypotheses are approximately independent and these C_k^2 association hypotheses can all pass the association hypothesis decision. Then, $P(B_k)$ can be approximated as follows:

$$P(B_k) \approx C_i^k P_{\mathrm{Ass}}^{C_k^2} (1-P_{\mathrm{Ass}})^{C_i^2 - C_k^2}. \tag{10}$$

The low-precision track confirmation is still used the 2/2 logic method. Thus, $P(C_k)$ can be expressed as follows:

$$P(C_k) = 1 - (1 - P_d P_{\mathrm{Threshold}})^k. \tag{11}$$

In fact, the event D_i indicates that the event B_k and event C_k occur at the same time. Therefore, we can calculate $P(D_i)$as follows:

$$P(D_i) = \sum_{k=2}^{i} P(B_k) P(C_k). \tag{12}$$

We assume that event A_i and event D_i are approximately independent. The probability $P_{\mathrm{Init-high}}^{(1)}$ of converting low-precision tracks into high-precision track can then be approximated as follows:

$$P_{\mathrm{Init-high}}^{(1)} \approx \sum_{i=2}^{N} P(A_i) P(D_i). \tag{13}$$

2) Probability of High-Precision Track Conformation by Remaining Secondary Measurements: The probability of occurrence of events E_i is related to event B_k and event C_k. This relationship can be expressed as follows:

$$P(E_i) = \sum_{k=2}^{i} P(B_k)(1 - P(C_k)). \tag{14}$$

Therefore, the 2/2 logic method, the probability $P_{\mathrm{Init-high}}^{(2)}$ of the remaining secondary measurement for the high-precision track conformation is

$$P_{\mathrm{Init-high}}^{(2)} = P_L P_{\mathrm{Threshold}} \cdot \sum_{i=2}^{N} P(A_i) P(E_i). \tag{15}$$

TABLE I
PROBABILITY $P_{\text{INIT-LBTI}}$ FOR 2/2 LBTI

P_d / N	0.7		0.8		0.9	
	THEORETICAL	SIMULATION	THEORETICAL	SIMULATION	THEORETICAL	SIMULATION
2	0.2059	0.2107	0.3515	0.3681	0.5625	0.5880
3	0.5515	0.5460	0.7320	0.7314	0.8751	0.8867
4	0.7747	0.7828	0.8848	0.9050	0.9383	0.9697

Theoretical calculation results refer to (9) with $P_{\text{Ass}} = 0.95$ and $P_{\text{Threshold}} = 0.95$. The number of bistatic pairs N from 2 to 4 and the detection probability P_{d} from 0.7 to 0.9.

TABLE II
PROBABILITY $P_{\text{INIT-LBTI}}$ FOR PROPOSED ALGORITHM

P_d / N	0.7		0.8		0.9	
	THEORETICAL	SIMULATION	THEORETICAL	SIMULATION	THEORETICAL	SIMULATION
2	0.4248	0.4176	0.5811	0.5771	0.7550	0.7590
3	0.7278	0.6988	0.8577	0.8452	0.9494	0.9488
4	0.8782	0.8678	0.9497	0.9515	0.9817	0.9913

Theoretical calculation results refer to (16) with $P_{\text{Ass}} = 0.95$ and $P_{\text{Threshold}} = 0.95$. The number of bistatic pairs N from 2 to 4 and the detection probability P_{d} from 0.7 to 0.9.

3) Total Probability of High-Precision Track Conformation: After the above calculation, the Total probability $P_{\text{Init}-\text{high}}$ of high-precision track conformation is calculated as follows:

$$P_{\text{Init}-\text{high}} = P^{(1)}_{\text{Init}-\text{high}} + P^{(2)}_{\text{Init}-\text{high}}. \tag{16}$$

In order to verify the correctness of the above theoretical derivation, 100 000 MC simulation results were used for comparison.

Tables I and II give the theoretical and simulation results of the 2/2 LBTI algorithm and the proposed algorithm respectively. The theoretical calculation results in both tables are in good agreement with the simulation results. The higher probability means the better performance of the track confirmation. Comparing the two tables, we can find that the performance of the two algorithms is positive correlation to the number of bistatic pairs and the detection probability. The performance in terms of the fast track conformation of the proposed algorithm is significantly better than the LBTI method when the number of bistatic pairs is small and the detection probability is low.

It should be noted that the use of the *M*/*N* logic for the initialization of the high-precision and low-precision tracks herein is to facilitate the above quantitative analysis. It does not mean that we have to initialize the tracks using the *M*/*N* logic in the proposed algorithm. In theory, similar conclusions can be obtained when other track initialization approaches are applied to the proposed algorithm. The essential reason why the proposed algorithm performs better in terms of the fast track conformation lies in that the low-precision track retains additional information and can be converted into the high-precision track under certain conditions.

B. Track Continuity and Accuracy

This part will evaluate the track continuity and accuracy of the high-precision track via MC simulations. In the simulations, there are three transmitters locate at *T*1 [–5000 m, 10 000 m], *T*2 [11 000 m, –8000 m], and *T*3 [15 000 m, 20 000 m] and the two receivers located at *R*1 [0 m, 0 m], *R*2 [–5000 m, –5000 m]. The typical accuracies of the bistatic range, bistatic velocity, and azimuth are 40 m, 1 m/s, and 3°, respectively. Assume that all bistatic pairs have the same detection probability. False alarms per frame are generated by a Poisson process with a mean 50 and uniformly distributed in the detection area. The LBTI method is used to initialize both low-precision track and high-precision track. The period of measurements update is 1 s and the simulation duration is 100 s.

The simulations mainly analyze the performance of the proposed algorithm in the case of insufficient bistatic pairs and low detection probability. There are three targets, as shown in Fig. 3. Considered two cases with $N = 2$, $P_{\text{d}} = 0.9$, and $N = 4$, $P_{\text{d}} = 0.7$. Here, the optimal sub-pattern assignment (OSPA) distance proposed in [30] is used as a performance measure. The advantage of the OSPA distance is that it not only calculates the position error of the track but also penalizes the false alarms or missed tracks. Here, the parameters in the OSPA distance are set as follows. The order of the norm is $p = 2$, the critical distance is $c = 200$. Two measurement fusion algorithms are used to characterize the tracking performance of the typical centralized estimation algorithm. One of the algorithms is the hypothesis decision (AHD) algorithm proposed in [27], the other is based on the *M*/*N* LBTI algorithm and Kalman filter (*M*/*N*–*KF*). The *M*/*N*–*KF* algorithm uses the *M*/*N* LBTI algorithm and a nonlinear Kalman filter to initialize new tracks and update the maintenance tracks, respectively. 100 MC simulations are performed.

The simulation results with three targets and $N = 2$,$P_{\text{d}} = 0.9$ are shown in Figs. 3 and 4. The two bistatic pairs are *T*1–*R*1 and *T*2–*R*1. Fig. 3 shows one MC simulation tracking results of the AHD algorithm, *M*/*N*–*KF* algorithm, and proposed algorithm, respectively. Compared with the truth, the proposed algorithm can continuously track all target when the number of bistatic pairs is small. At this time, the tracks obtained by AHD algorithm are not continuous. Fig. 4 shows the OSPA distance and the average number of targets versus time. In Fig. 4(b), the average number of tracks of the three algorithms does not exceed the number of real targets, indicating that all these algorithms can perform well in clutter environment. The average number of tracks obtained by the AHD algorithm is significantly lower than the other two algorithms. The penalty in OSPA metric leads to far larger OSPA as shown in Fig. 4(a). The reason is that the target can be located only when it is detected by both bistatic pairs. When only one bistatic pair detects the target, the

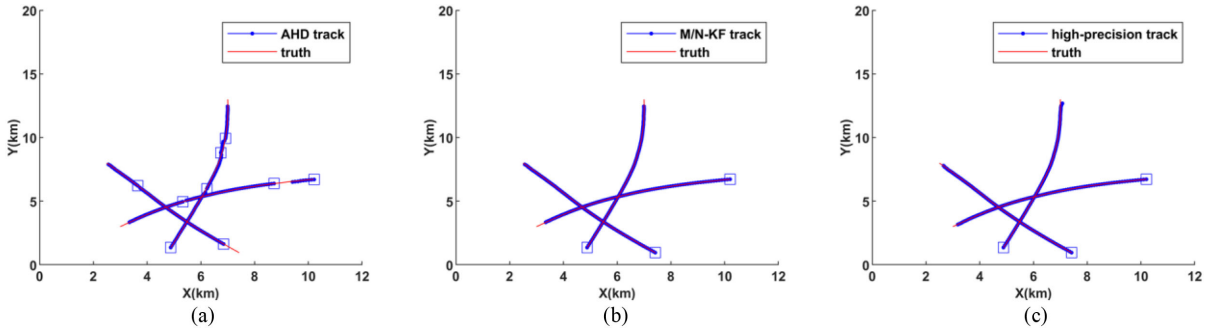

Fig. 3. Target tracks of one simulation with three targets and $P_{\rm d} = 0.9$, $N = 2$. A square is plotted at the terminal of each track. (a) Tracks obtained by AHD algorithm. (b) Tracks obtained by M/N-KF algorithm. (c) Tracks obtained by proposed algorithm.

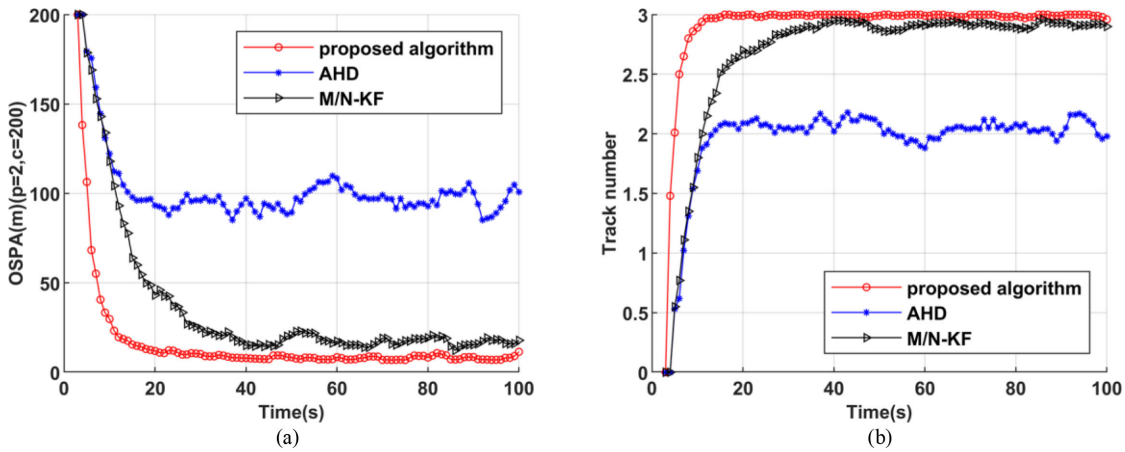

Fig. 4. 100 MC average track number and OSPA distance versus time with three targets and $P_{\rm d} = 0.9$, $N = 2$. (a) OSPA. (b) Track number.

AHD algorithm cannot update the track, causing the track to be interrupted. As indicated in Fig. 4(a), when the OSPA distance tends to be stable, the *M/N–KF* algorithm yields slightly larger results than the proposed algorithm. The main reason is that the proposed algorithm can quickly initialize the target track again after the target is interrupted. It should also be noted that the OSPA distance of the proposed algorithm converges faster than the AHD and *M/N–KF* algorithm, which indicates that the proposed algorithm has faster high-precision track confirmation ability. This phenomenon is consistent with the discussion in Section IV-A.

Next, we consider the case with three targets and $N = 4$, $P_d = 0.7$. The four bistatic pairs are *T*1–*R*1, *T*1–*R*2, *T*2–*R*1, and *T*2–*R*2. The simulation results are plotted in Fig. 5. For the proposed algorithm, the average number of tracks basically matches the number of real targets and the OSPA distance also converges faster than the other two algorithms.

Fig. 6 shows the root mean square error (RMSE) of the position and velocity of the proposed algorithm in the case of various number of bistatic pairs. Since we only care about the accuracy of the track, we set the detection probability and false alarms to 1 and 0, respectively. The RMSE is calculated as

$$\mathrm{RMSE} = \sqrt{\sum_{s=1}^{S} (\Delta x_s^2 + \Delta y_s^2)/S} \tag{17}$$

where S is the number of MC simulations, Δx_s and Δy_s represent the error in the x and y direction in the sth $(s = 1, 2, \cdots, S)$ simulation, respectively. The number of the bistatic pairs is 2 to 5. The results show that the RMSEs of the position and velocity converge to less than 10 m and 1 m/s, respectively. The more bistatic pairs, the lower RMSEs of the position and velocity.

V. Field Experimental Results

The field experimental data, which was acquired in September 2018 by Wuhan University in the northwest of China, is employed to verify the practical feasibility of the proposed algorithm. The selected duration was about 5 min. A quadrotor drone with a diameter of about 0.5 m is used as the cooperative target. The data period is 1 s. The scenario of the MPR configuration is depicted in Fig. 7. There are two transmitters and one receiver. The transmitters *Tx*1 and *Tx*2 transmit digital television terrestrial multimedia broadcasting signal in 626 and 746 MHz,

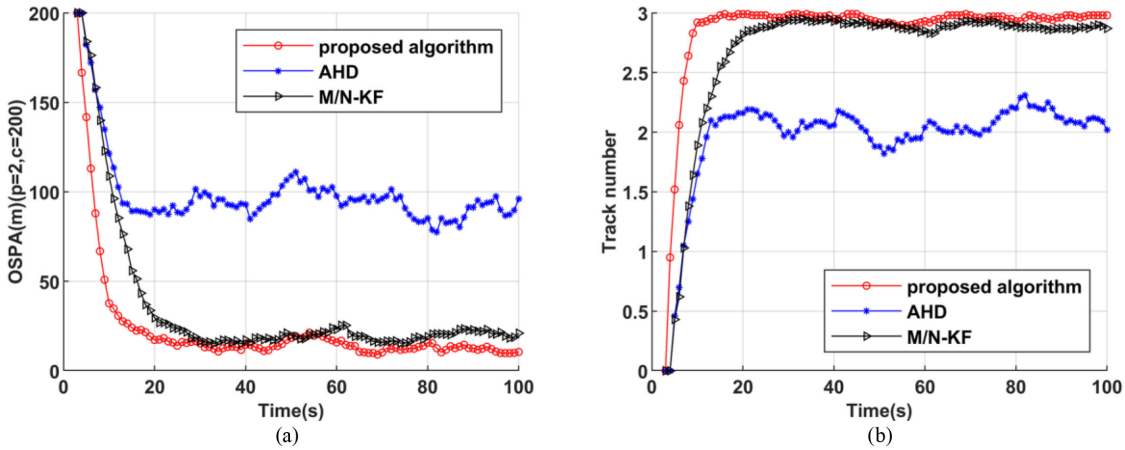

Fig. 5. 100 MC average track number and OSPA distance versus time with three targets and $P_{\mathrm{d}} = 0.7$, $N = 4$. (a) OSPA. (b) Track number.

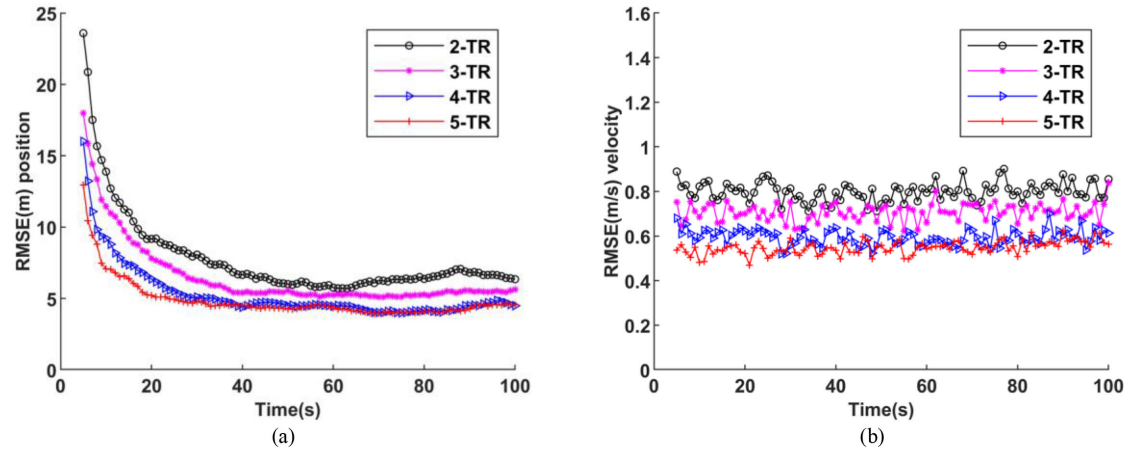

Fig. 6. 100 MC RMSE of position and velocity with $N = 2$ to $N = 5$. (a) RMSE of position. (b) RMSE of velocity.

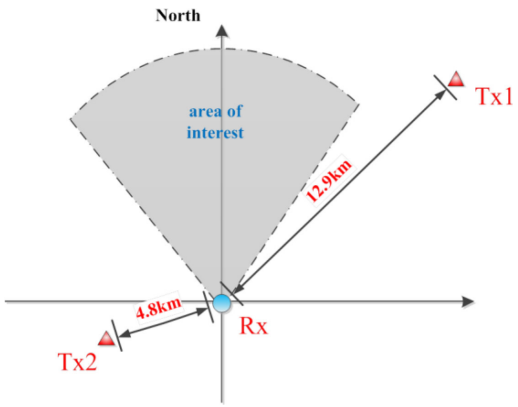

Fig. 7. Multistatic passive radar configuration in the northwest of China, one receiver, two transmitters, and the area of interest.

respectively. The receiver *Rx* receives the signals from both the transmitters *Tx*1 and *Tx*2. The position information of the drone recorded by the global positioning system (GPS) is used as the reference.

Fig. 8(a) shows the track results of the first bistatic pair. Apart from the target tracks, there are many other tracks, which may be originated from birds, cars, and even other noncooperative drones. Regarding the target track, it is not continuous. Compared with the GPS, the track error is relatively large. Fig. 8(b) shows the processing results of the other bistatic pair. This result is slightly better than Fig. 8(a) in the track continuity and accuracy.

Fig. 9 shows the fusion results of the two bistatic pairs. The results of all the three algorithms are given here. We only focus on the track results of the cooperative target. Fig. 9(a) shows the tracking result of the AHD algorithm. The performance of the AHD algorithm is worse than the other two algorithms in the track continuity. Fig. 9(b) and (c) show the tracking results of the *M*/*N*–*KF* algorithm and proposed algorithm, respectively. Compared with GPS, both algorithms seem to perform well in terms of the track continuity and accuracy. Note that the track discontinuity marked by green circle in Fig. 8(b) is caused by the hovering behavior of the drone. The proposed algorithm can initialize the target track faster when the drone starts moving again. We use the target's position recorded by the GPS as the

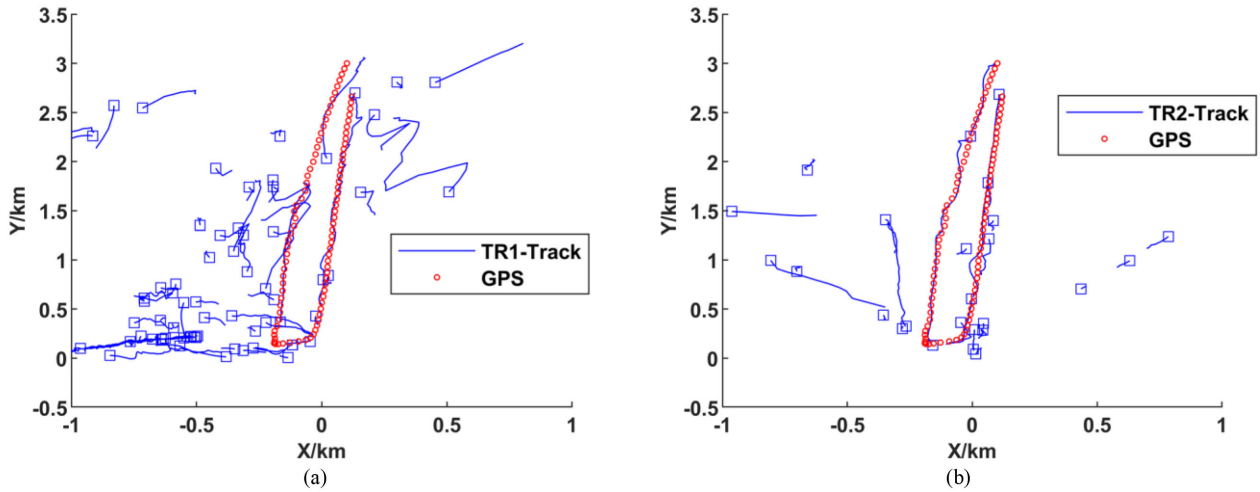

Fig. 8. Target tracks of each bistatic pair. A square is plotted at the terminal of each track. (a) Tracks of the first bistatic pair. (b) Tracks of the second bistatic pair.

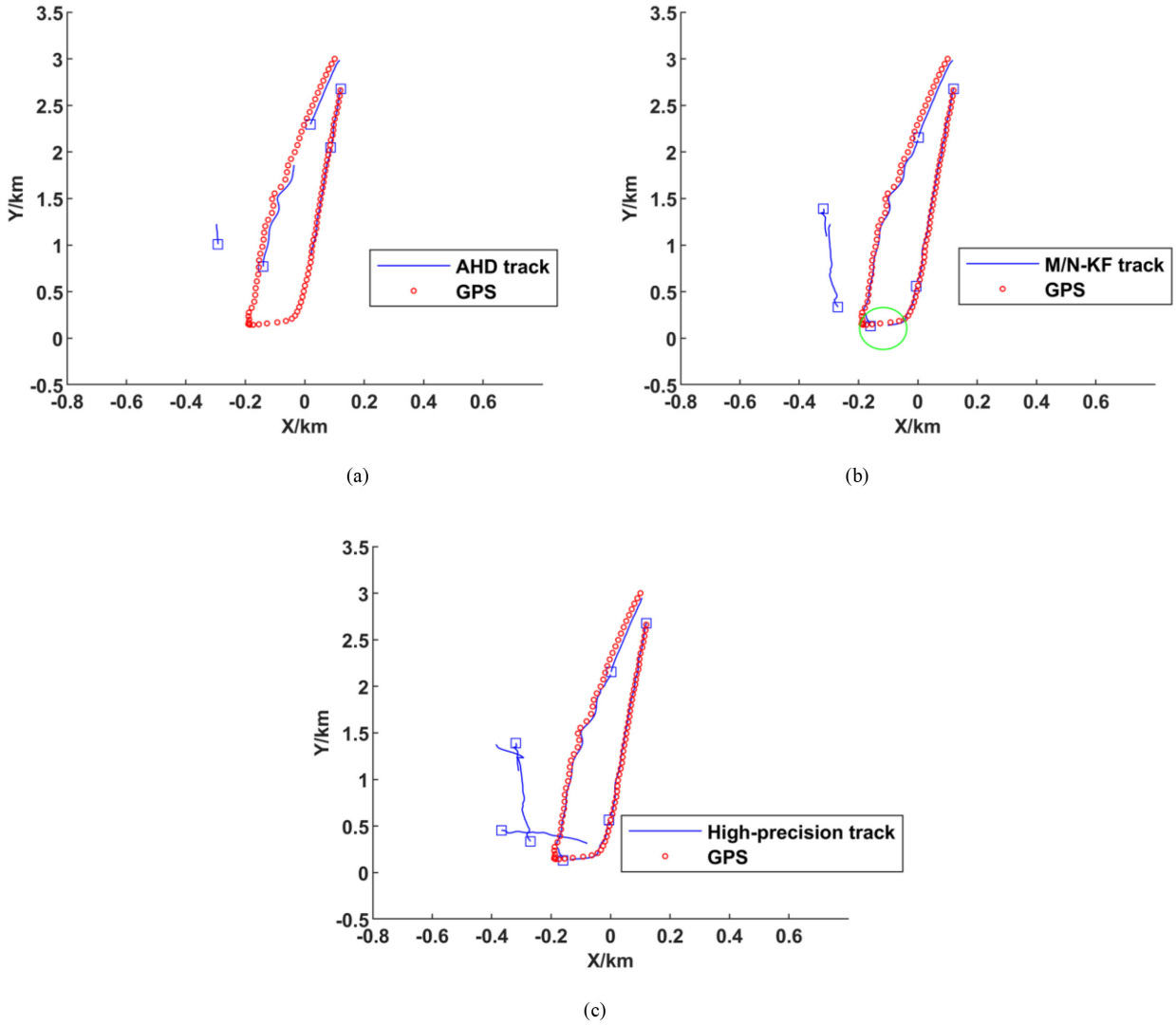

Fig. 9. Tracks fused from both two bistatic pairs. (a) Tracks obtained by the AHD algorithm. (b) Tracks obtained by the *M/N-KF* algorithm. (c) Tracks obtained by the proposed algorithm.

reference to count the position error. The RMSE of the target's position estimate by proposed algorithm is about 22 m.

VI. Conclusion

We proposed a hybrid tracking algorithm for the MPR in this article. In the MPR, the existing tracking algorithms face problems in the fast track confirmation, track continuity, and accuracy in the case of insufficient bistatic pairs and low detection probability. We construct the high-precision track and low-precision track to handle these problems. Theoretical analyses show that even if the number of bistatic pairs is only set to 2, the proposed algorithm can still significantly increase the probability of high-precision track confirmation compared with the LBTI algorithm. It is also shows that the proposed algorithm performs well in terms of the track continuity and accuracy in clutter environment. The practicability of the proposed algorithm is also validated using real data. With the development of the MPR, asynchronous sensor fusion is imperative. However, most of the existing measurement fusion methods are based on time synchronization. Our future work is to develop an asynchronous sensor fusion strategy based on measurement fusion method.

References

[1] P. E. Howland, D. Maksimiuk, and G. Reitsma, "FM radio based bistatic radar," *IEEE Pro. Radar Sonar Navig.*, vol. 152, no. 3, pp. 107–115, Jun. 2005.

[2] H. D. Griffiths and C. J. Baker, "Passive coherent location radar systems. Part 1: Performance prediction," *IEEE Pro. Radar Sonar Navig.*, vol. 152, no. 3, pp. 153–159, Jun. 2005.

[3] P. E. Howland, "Target tracking using television-based bistatic radar," *IEEE Pro. Radar Sonar Navig.*, vol. 146, no. 3, pp. 166–174, Jun. 1999.

[4] J. Yi, X. Wan, D. Li and H. Leung, "Robust clutter rejection in passive radar via generalized subband cancellation," *IEEE Trans. Signal Process.*, vol. 54, no. 4, pp. 1931–1946, Aug. 2018.

[5] E. Fishler, A. Haimovich, R. Blum, D. Chizhik, L. Cimini and R. Valenzuela, "MIMO radar: An idea whose time has come," in *Proc.IEEE Radar Conf.*, 2004, pp. 71–78.

[6] G. Fang, J. Yi, X. Wan, Y. Liu, and H. Ke, "Experimental research of multistatic passive radar with a single antenna for drone detection," *IEEE Access*, vol. 6, pp. 33542–33551, 2018.

[7] J. Yi, X. Wan, H. Leung, and M. Lü, "Joint placement of transmitters and receivers for distributed MIMO radars," *IEEE Trans. Aerosp. Electron. Syst.*, vol. 53, no. 1, pp. 122–134, Feb. 2017.

[8] D. E. Hack, L. K. Patton, B. Himed, and M. A. Saville, "Detection in passive MIMO radar networks," *IEEE Trans. Signal Process.*, vol. 62, no. 11, pp. 2999–3012, Jun. 2014.

[9] Y. Bar-Shalom and W. D. Blair, *Multitarget-Multisensor Tracking: Applications and Advances*. Boston, MA, USA: Artech House, 2000.

[10] Y. Bar-Shalom, P. Willett, and X. Tian, *Tracking and Data Fusion: A Handbook of Algorithms*. Bloomfield, CT, USA: YBS Publishing, 2011.

[11] K. C. Chang, R. K. Saha, and Y. Bar-Shalom, "On optimal track-to-track fusion," *IEEE Trans. Aerosp. Electron. Syst.*, vol. 33, no. 4, pp. 1271–1276, Oct. 1997.

[12] K. C. Chang, C-Y. Chong, and S. Mori, "Analytical and computational evaluation of scalable distributed fusion algorithms," *IEEE Trans. Aerosp. Electron. Syst.*, vol. 46, no. 4, pp. 2022–2034, Oct. 2010.

[13] C. Chong, "Forty years of distributed estimation: A review of noteworthy developments," in *Proc. Sensor Data Fusion, Trends, Solutions, Appl.*, 2017, pp. 1–10.

[14] Y. Bar-Shalom, "On hierarchical tracking for the real world," *IEEE Trans. Aerosp. Electron. Syst.*, vol. 42, no. 3, pp. 846–850, Jul. 2006.

[15] P. W. Moo and Z. Ding, "Tracking performance of MIMO radar for accelerating targets," *IEEE Trans. Signal Process.*, vol. 61, no. 21, pp. 5205–5216, Nov. 2013.

[16] X. Gao, J. Chen, D. Tao, and X. Li, "Multi-sensor centralized fusion without measurement noise covariance by variational bayesian Approximation," *IEEE Trans. Aerosp. Electron. Syst.*, vol. 47, no. 1, pp. 718–272, Jan. 2011.

[17] M. Daun, U. Nickel, and W. Koch, "Tracking in multistatic passive radar systems using DAB/DVB illumination," *Signal Process.*, vol. 92, no. 6, pp. 1365–1386, 2012.

[18] B. Balakumar, S. Shahbazpanahi, and T. Kirubarajan, "Joint MIMO channel tracking and symbol decoding using kalman filtering," *IEEE Trans. Signal Process.*, vol. 55, no. 12, pp. 5873–5879, Dec. 2007.

[19] H. Chen, T. Kirubarajan and Y. Bar-Shalom, "Performance limits of track-to-track fusion versus centralized estimation: theory and application [sensor fusion]," *IEEE Trans. Aerosp. Electron. Syst.*, vol. 39, no. 2, pp. 386–400, Apr. 2003.

[20] M. Malanowski and K. Kulpa, "Two methods for target localization in multistatic passive radar," *IEEE Trans. Aerosp. Electron. Syst.*, vol. 48, no. 1, pp. 572–580, Jan. 2012.

[21] A. Noroozi and M. A. Sebt, "Target localization in multistatic passive radar using SVD approach for eliminating the nuisance parameters," *IEEE Trans. Aerosp. Electron. Syst.*, vol. 53, no. 4, pp. 1660–1671, Aug. 2017.

[22] B. K. Chalise, Y. D. Zhang, M. G.Amin, and B. Himed, "Target localization in a multi-static passive radar system through convex optimization," *Signal Process.*, vol. 102, no. 6, pp. 207–215, 2014.

[23] R. Tharmarasa, M. Subramaniam, N. Nadarajah, T. Kirubarajan and M. McDonald, "Multitarget passive coherent location with transmitter-origin and target-altitude uncertainties," *IEEE Trans. Aerosp. Electron. Syst.*, vol. 48, no. 3, pp. 2530–2550, Jul. 2012.

[24] R. Amiri, F. Behnia, and H. Zamani, "Asymptotically efficient target localization from bistatic range measurements in distributed MIMO radars," *IEEE Signal Process. Lett.*, vol. 24, no. 3, pp. 299–303, Mar. 2017.

[25] M. Klein and N. Millet, "Multireceiver passive radar tracking," *IEEE Areosp. Electron. Syst. Mag.*, vol. 27, no. 10, pp. 26–36, Oct. 2012.

[26] M. Lü, X. Wan, J. Yi, and F. Cheng, "New method of target track maintenance in single frequency network based passive radar," *J. Syst. Eng. Electron.*, vol. 39, no. 9, pp. 1965–1970, Sep. 2017.

[27] J. Yi, X. Wan, H. Leung, and F. Cheng, "MIMO passive radar tracking under a single frequency network," *IEEE J. Sel. Top. Signal Process.*, vol. 9, no. 8, pp. 1661–1671, Dec. 2015.

[28] S. Choi, D. F. Crouse, P. Willett, and S. Zhou, "Approaches to cartesian data association passive radar tracking in a DAB/DVB network," *IEEE Trans. Aerosp. Electron. Syst.*, vol. 50, no. 1, pp. 649–663, Jan. 2014.

[29] Z. Hu, H. Leung, and M. Blanchette, "Statistical performance analysis of track initiation techniques," *IEEE Trans. Signal Process.*, vol. 45, no. 2, pp. 445–456, Feb. 1997.

[30] D. Schuhmacher, B. Vo, and B. Vo, "A consistent metric for performance evaluation of multi-object filters," *IEEE Trans. Signal Process.*, vol. 56, no. 8, pp. 3447–3457, Aug. 2008.

[31] M. Malanowski, K. Kulpa and R. Suchozebrski, "Two-stage tracking algorithm for passive radar," in *Proc. 12th Int. Conf. Inf. Fusion*, 2009, pp. 1800–1806.

[32] J. Yi, X. Wan, F. Cheng, Z. Zhao, and H. Ke, "Deghosting for target tracking in single frequency network based passive radar," *IEEE Trans. Signal Process.*, vol. 51, no. 4, pp. 2655–2668, Oct. 2015.

[33] A. A. Konovalov, "Target tracking algorithm for passive coherent location," *IET Radar, Sonar Navigation*, vol. 10, no. 7, pp. 1228–1233, 2016.

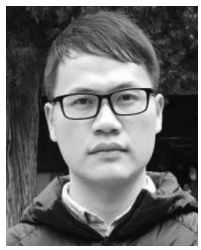

Kan Shu was born in Hubei, China, in 1992. He received the B.E. degree in communication engineering from South-Central University for Nationalities, Wuhan, China, in 2015. He is currently working toward the Ph.D. degree with the School of Electronica Information, Wuhan University, Wuhan, China.

His research interests include target tracking and information fusion.

Jianxin Yi (Member, IEEE) received the B.E. degree in electrical and electronic engineering, and the Ph.D. degree in radio physics from Wuhan University, Wuhan, China, in 2011 and 2016, respectively, and the Ph.D. degree from the University of Calgary, Calgary, AB, Canada.

He is currently an Assistant Professor with the School of Electronic Information, Wuhan University. He has been supported by the Postdoctoral Innovation Talent Support Program of China. His main research interests include radar signal processing, target tracking, and information fusion.

Dr. Yi was the recipient of the 2017 Excellent Doctoral Dissertation Award from the Chinese Institute of Electronics.

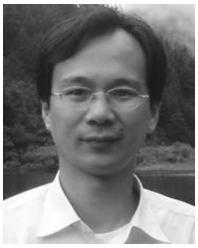

Xianrong Wan received the B.E. degree from the former Wuhan Technical University of Surveying and Mapping, Wuhan, China, in 1997, and the Ph.D. degree from Wuhan University, Wuhan, China, in 2005.

He is currently a Professor and the Ph.D. Candidate Supervisor with the School of Electronic Information, Wuhan University. In recent years, he has hosted and participated in more than ten national research projects, and authored or coauthored more than 80 academic paper. His main research interests include design of new radar system such as passive radar, over-the-horizon radar, and array signal processing.

Feng Cheng received the B.E. degree in electrical and electronic engineering, and the Ph.D. degree in radio physics, from Wuhan University, Wuhan, China, in 1998 and 2006, respectively.

He is currently an Associate Professor with Wuhan University. His main research interests include radar signal processing, radio ocean remote sensing, and radar software engineering.